# Kolmogorov turbulence defeated by Anderson localization

Dima Shepelyansky (CNRS, Toulouse)
www.quantware.ups-tlse.fr/dima

with L.Ermann, E.Vergini (CNEA Buenos Aires) PRL **119**, 054103 (2017) + ...

532.507

**ЛОКАЛЬНАЯ СТРУКТУРА ТУРБУЛЕНТНОСТИ В НЕСЖИМАЕМОЙ ВЯЗКОЙ ЖИДКОСТИ ПРИ ОЧЕНЬ БОЛЬШИХ ЧИСЛАХ РЕЙНОЛЬДСА *)**

*А. Н. Колмогоров*

§ 1. Будем обозначать через

$$U_\alpha(P) = U_\alpha(x_1, x_2, x_3, t), \qquad \alpha = 1, 2, 3,$$

компоненты скорости в момент времени $t$ в точке с прямоугольными декартовыми координатами $x_1, x_2, x_3$. При изучении турбулентности естественно считать компоненты скорости $U_\alpha(P)$ в каждой точке $P = (x_1, x_2, x_3, t)$

*) ДАН СССР 30 (4), 299 (1941).

V.E. Zakharov V.S. L'vov
G. Falkovich

Kolmogorov Spectra of Turbulence I
Wave Turbulence

With 34 Figures

Springer-Verlag
Berlin Heidelberg New York
London Paris Tokyo
Hong Kong Barcelona
Budapest

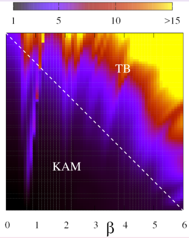


Kolmogorov (1941) - energy flow over space scales $E_k \propto 1/k^{5/3}$;
Zakharov-Filonenko (1967) capilary waves $E_k \propto 1/k^{7/4}$ $\rightarrow$ “In the theory of weak turbulence nonlinearity of waves is assumed to be small; this enables us, using the hypothesis of the random nature of the phase of individual waves, to obtain the kinetic equation for the mean square of the wave amplitudes”; extentions $\rightarrow$ Zakharov, L'vov, Falkovich(1992); Nazarenko(2011)

# Energy equipartition over degrees of freedom

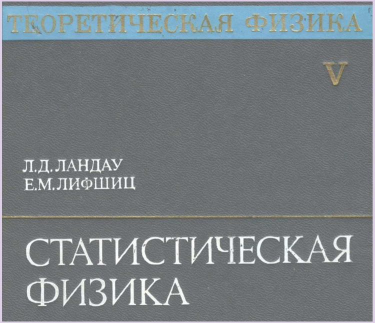


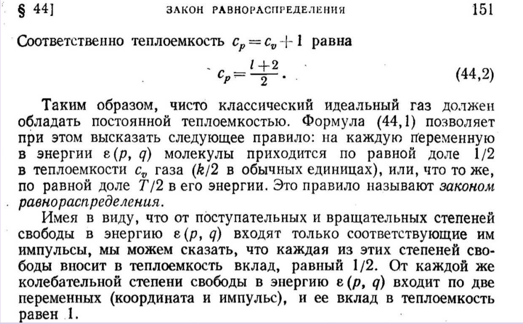

§ 44] ЗАКОН РАВНОРАСПРЕДЕЛЕНИЯ 151

Соответственно теплоемкость $c_p = c_v + 1$ равна

$$c_p = \frac{l+2}{2}. \qquad (44,2)$$

Таким образом, чисто классический идеальный газ должен обладать постоянной теплоемкостью. Формула (44,1) позволяет при этом высказать следующее правило: на каждую переменную в энергии $\varepsilon(p, q)$ молекулы приходится по равной доле 1/2 в теплоемкости $c_v$ газа ($k/2$ в обычных единицах), или, что то же, по равной доле $T/2$ в его энергии. Это правило называют *законом равнораспределения*.

Имея в виду, что от поступательных и вращательных степеней свободы в энергию $\varepsilon(p, q)$ входят только соответствующие им импульсы, мы можем сказать, что каждая из этих степеней свободы вносит в теплоемкость вклад, равный 1/2. От каждой же колебательной степени свободы в энергию $\varepsilon(p, q)$ входит по две переменных (координата и импульс), и ее вклад в теплоемкость равен 1.

Nauka Moscow (1976)

Dynamical thermalization in finite isolated systems?

Fermi-Pasta-Ulam (FPU) problem (1955)

Chirikov criterion for onset of chaos (1959)

Novosibirsk => FPU: Izrailev, Chirikov Dokl. Akad. Nauk SSSR 166: 57 (1966)

Integrability of nonlinear Schrödinger equation
Zakharov, Shabat, Zh. Eksp. Teor. Fiz. 61: 118 (1971) + Toda lattice (1967)

# Dynamical thermalization in finite systems

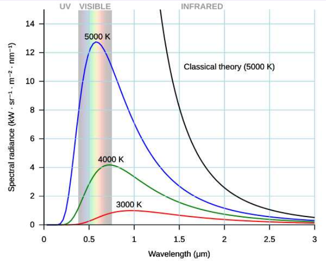


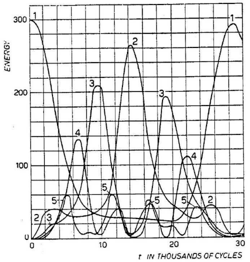


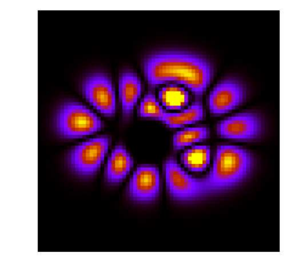

Planck's law (1900); Fermi-Pasta-Ulam problem (1955);
Bose-Einstein condensate (BEC) in Sinai-oscillator trap (2016) (left to right)
Ketterle group PRL (1995) => BEC in Sinai oscillator (not understood; 3d)

# Chaos in Sinai oscillator

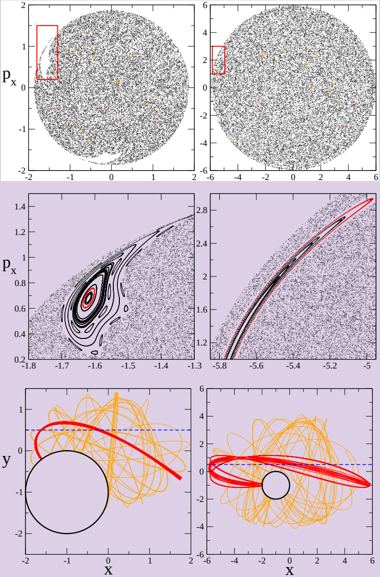


$H_S = (p_x^2 + p_y^2)/2 + x^2/2 + y^2$, disk $r_d = 1$ at $x = y = -1$; $E = 2, 18$ (left, right)

# BEC in Sinai oscillator

Gross-Pitaevskii equation (GPE or NSE)

The BEC evolution in the Sinai oscillator trap is described by the GPE, which reads as

$$i\hbar\frac{\partial\psi(\vec{r},t)}{\partial t} = -\frac{\hbar^2}{2m}\vec{\nabla}^2\psi(\vec{r},t) + \left[\frac{m}{2}(\omega_x^2x^2+\omega_y^2y^2)+V_d(x,y)\right]\psi(\vec{r},t) + \beta|\psi(\vec{r},t)|^2\psi(\vec{r},t). \quad (2)$$

Here in (2), we use the same oscillator and disk parameters as in (1) and take $\hbar = 1$. The wave function is normalized to unity $W = \int |\psi(x,y)|^2 dx\,dy = 1$. Then, the parameter $\beta$ describes the nonlinear interactions of atoms in BEC. All

# Quantum chaos in Sinai oscillator

Wigner-Dyson level spacing statistics

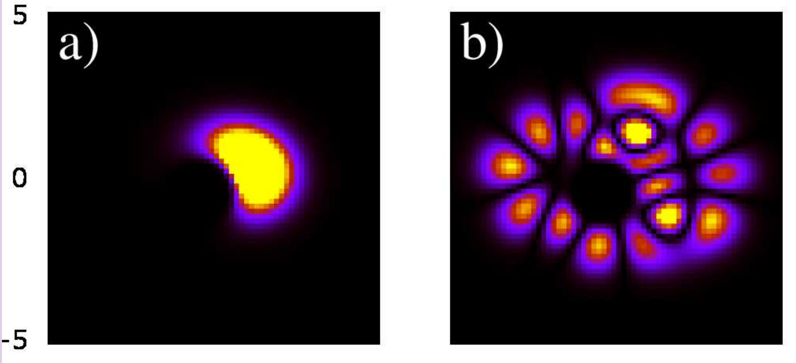


Eigenstates at $\beta = 0$; ground state $m = 1$ and $m = 24$

Bose-Einstein anzats: $\rho_m = 1/[\exp(E_m - E_g - \mu)/T) - 1]$;
$\rho_m =< |\psi_m|^2 >$, $\sum_m E_m \rho_m = E$, $S = -\sum_m \rho_m \ln \rho_m \rightarrow S(E)$

# Bose-Einstein anzats for dynamical thermalization

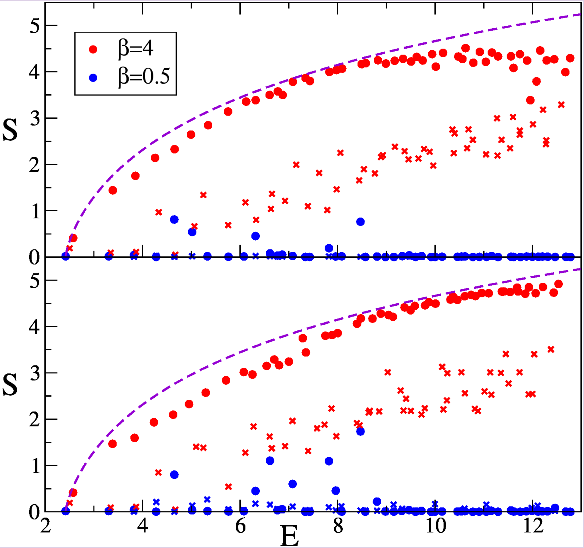


first 50 states; Sinai osc (dots), no disk (X); $500/1500 < t < 1500/2500$ (top/bottom); Bose-Einstein anzats (dashed) → no energy equipartition

# Bose-Einstein anzats

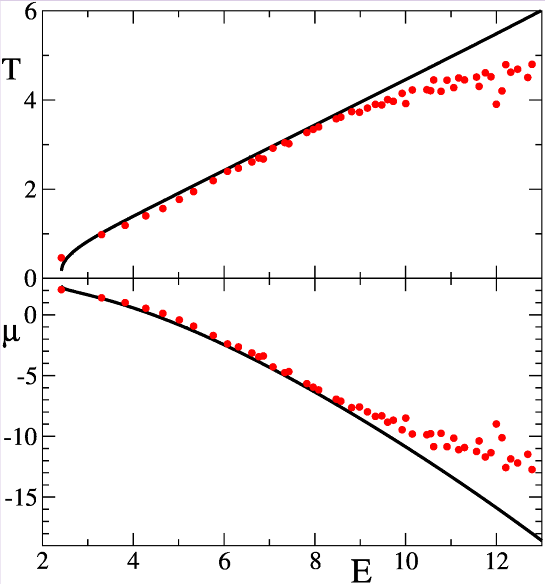


temperature and chemical potential dependence on energy ($\beta = 4$)

# BEC time evolution

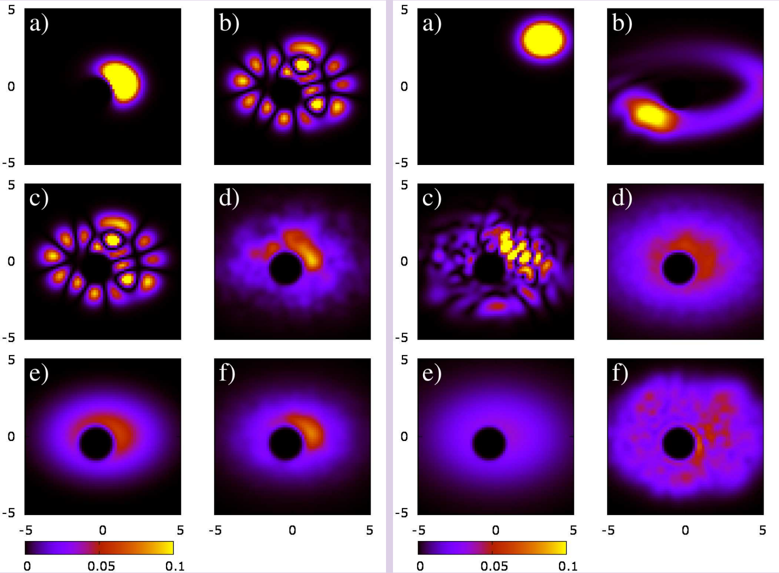


$\beta = 4$ various initial states

# BEC in Sinai-oscilator trap with driving

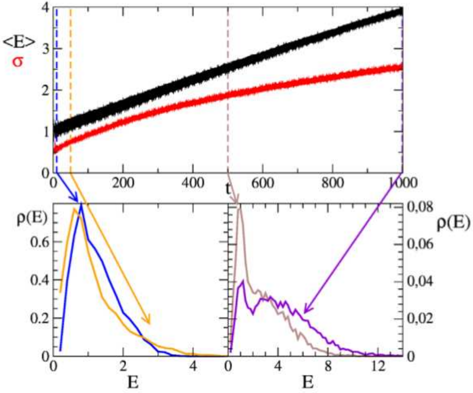


FIG. 1. Classical time evolution of average energy $\langle E \rangle$ and its standard deviation $\sigma$ for $f = 0.4$. The data are obtained from $10^4$ trajectories with random initial conditions at $\langle E \rangle = 1$ and $\sigma = 0.5$. Top panel: $\langle E(t) \rangle$ and $\sigma(t)$ are shown by black and red (gray) curves, respectively. Bottom panels show probability distribution of trajectories $\rho(E, t)$ for (a) $t = 10, 50$ [blue (black),

$H = H_S(x, y, p_x, p_y) + fx \sin \omega t$ (classical dynamics)

# Energy flow to high modes

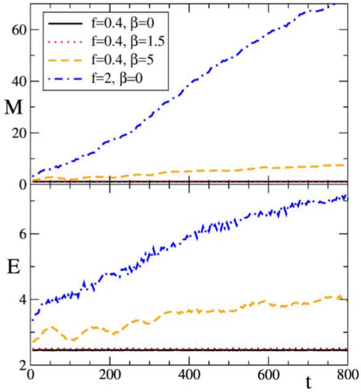


FIG. 2. Time evolution of $M$ (top panel) and energy $E$ (bottom panel) for GPE (2) averaged over time intervals $\Delta t = 1$. The initial state is the ground state of (2) at $\beta = 0$, $f = 0$ [see Fig. 5(a) in Ref. [28]]. Both panels show the cases of $f = 0.4, \beta = 0$ (black solid lines), $f = 0.4$, $\beta = 1.5$ [red (gray) dotted lines], $f = 0.4$, $\beta = 5$ [orange(gray) dashed lines], $f = 2, \beta = 0$ [blue (gray) dot-dashed lines].

$M = \sum_k k\rho_k$; $\ell_\phi \approx 2\pi\rho_c(D/\omega)^2 \approx 2f^2{\omega_x}^2 E^{3/2}/\omega^4$ (ground state);
Anderson photonic localization $\rho_k \propto \exp(-2E/\omega\ell_\phi)$ for $\beta = 0$, $f < f_c \approx 1.5$

# Energy flow to high modes

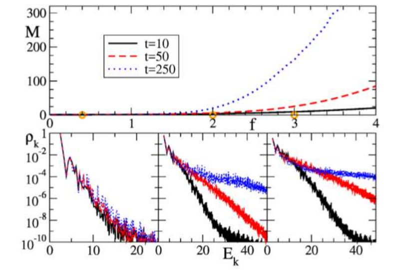


FIG. 3. Top panel shows $M$ as a function of driven force $f$ for linear case ($\beta = 0$). Bottom panels show probability distribution $\rho_k$, averaged over time interval $\Delta t = 5$, as a function of eigenenergies $E_k$ with $t = 10$ in black solid lines, $t = 50$ in the red (gray) dashed lines, and $t = 250$ in blue (gray) dotted lines. Left, center, and right bottom panels show the cases of $f = 0.4$, 2, and 3, respectively [highlighted with orange (gray) circles in top panel].

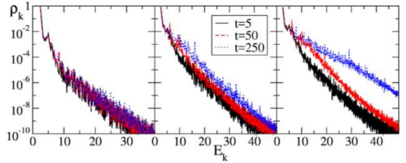


FIG. 4. Same as in bottom panels of Fig. 3 for $f = 0.3$, $\beta = 1.5$ (left panel); $f = 0.5, \beta = 5$ (center panel); $f = 1, \beta = 5$ (right panel).

$M$ and probability distributions $\rho_k$; left $\rightarrow \beta = 0$;
right $f = 0.3, \beta = 1.5$, $f = 0.5, \beta = 5$, $f = 1, \beta = 5$

# Turbulence phase diagram

$$f_c r_d/\hbar\omega_x \approx 1.5[1 - \beta_c/(6\hbar\omega_x {r_d}^2)] \qquad (3)$$

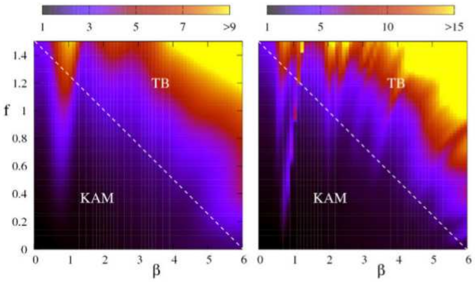


FIG. 5. Number of modes $M$ shown by color (grayness) in the plane of parameters $f$ and $\beta$ (average is done in the time intervals $100 \le t \le 150$ and $250 \le t \le 300$ in left and right panels, respectively). The approximate separation of KAM or insulator phase (KAM) and delocalized turbulent or metallic phase (TB) is shown by the white line (3).

Thus there is a stability domain where the Kolmogorov flow from large to small scales is defeated by the Anderson localization and KAM-integrability

# Quantware Localization Kaleidoscope

$$\mathrm{i}\frac{\partial \psi_{n_x n_y}}{\partial t} = E_{n_x n_y}\psi_{n_x n_y} + \beta|\psi_{n_x n_y}|^2\psi_{n_x n_y} + (\psi_{n_x+1 n_y} + \psi_{n_x-1 n_y} + \psi_{n_x n_y+1} + \psi_{n_x n_y-1}). \quad (6)$$

Periodic boundary conditions are used for the $N \times N$ square lattice with $-N/2 \leqslant n_x, n_y \leqslant N/2$. However, here we use the extended version of this model assuming that

$$E_{n_x n_y} = \delta E_{n_x n_y} + f(n_x^2 + n_y^2), \quad -W/2 \leqslant \delta E_{n_x n_y} \leqslant W/2 \ (M3). \quad (7)$$

This is the $M3$ model with random values of energies $\delta E_{n_x n_y}$ in a given interval.

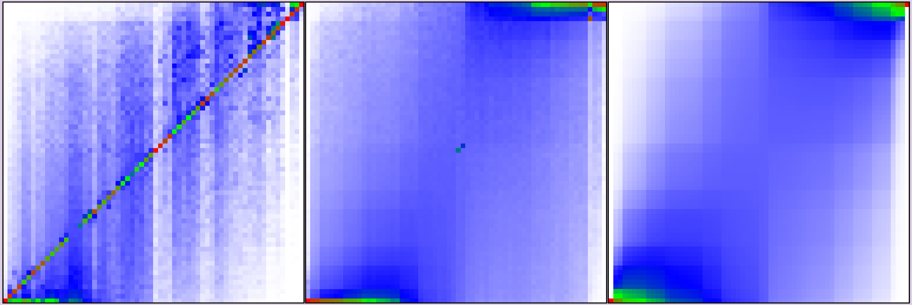

Nonlinear chains with disorder: $8 \times 8$ sites, $f = 1$, $W = 2$, $\beta = 1, 4$ (left, center); quantum Gibbs anzats (right); $t = 2 \times 10^6$ (Ermann, DS NJP (2013))

# Quantware Localization Kaleidoscope

Two interaction particles (TIP) in 1d Anderson model: K.Frahm EPJB (2016)

Eur. Phys. J. B (2016) 89: 115

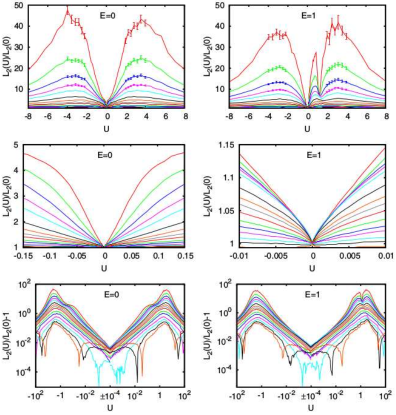


**Fig. 15.** Dependence of $L_2(U)/L_2(0)$ on $U$ for $E = 0$ (left panels) and $E = 1$ (right panels) and the disorder values $W$ used in Figure 11 with $W = 0.5$ for the top red curves and increasing values of $W$ corresponding to decreasing curves. Here $L_2(U)$ represents the infinite size localization length obtained by finite size scaling for the interaction strength $U$. Top panels

# Quantware Localization Kaleidoscope

TIP in 1d (fig), 2d Harper model: Frahm, DS EPJB (2015), (2016)

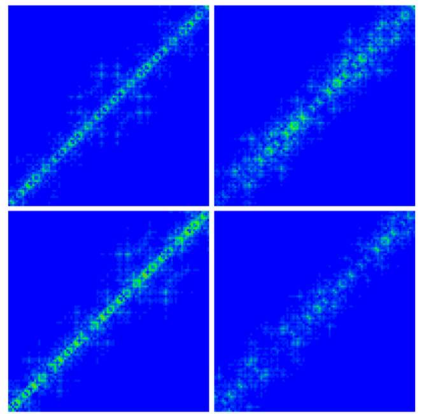

Total lattice size $N = 10946$, Harper amplitude $\lambda = 2.5 > 2$ (localized phase); TIP eigenstates at Hubbard interaction $U = 4.5$ (left), $U = 7.8$ (right); zoom $100 \times 100$ at $x = 0$; $x = 5000$.

# Quantware Localization Kaleidoscope

Anderson transition for Google matrix eigenstates
(Zhirov, DS Ann. der Phys. (2015))

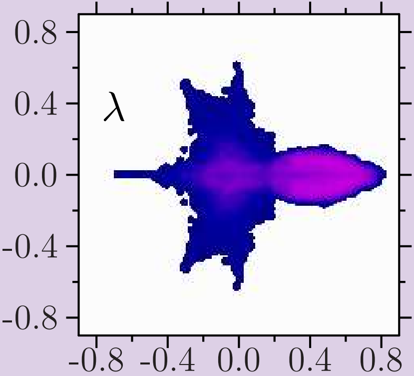


Google matrix with complex spectrum $\lambda$ and IPR values of eigenstates ($N = 19600$), mobily edge in a complex plane ?

# Quantware Localization Kaleidoscope

Quantum chaos of dark matter in the Solar System (DS arXiv (2017))

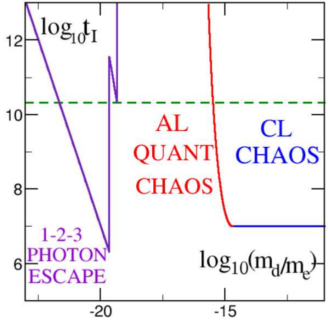


FIG. 2: (Color online) Dependence of DMP escape (ionization) time $_I$ from the SS as a function of mass ration $m_d/m_e$ for initial DMP energy $E_d = -m_d {v_J}^2/2$. The blue/black horizontal line shows regime of classical escape due to chaos, red/gray curve shows $t_I$ (9) in the regime of Anderson localization of quantum photonic transitions, violet line shows $t_i$ (10) in the regime of 1,2 and 3 photon escape; horizontal dashed line marks the life time of Universe $t_U$.

Anderson photonic localization for $m_d/m_e < 2 \times 10^{-15}$; localization length in number of Jupiter photons is $\ell_\phi \approx 2 \times 10^{34}(m_d/m_e)^2$.

# Discussion

Interplay of Anderson localization and interactions?

Interplay of Anderson localization and nonlinearity?

Conditions of dynamical thermalization?

not too weak and not too strong interactions

Åberg criterion: two-body matrix element should be larger than the spacing between directly coupled states

S.Åberg PRL **64**, 3119 (1990); later Jacquod, DS PRL (1997)

(now called Many-Body Localization (MBL) and Eigenstate Thermalization Hypothesis (ETH))

New twist: Dynamical localization for quantum dots and SYK black holes (Kolovsky, DS EPL (2016))
quantum dot $\rightarrow \delta E \approx g^{2/3}\Delta$
SYK black hole $\rightarrow$?